CHAPTER VIII

DATA REDUCTION

By Sheldon Kopelson
Langley Research Center

SECTION I - INTRODUCTION

A large volume of data were generated both during the development program and the flight lifetime of the Explorer XIII Micrometeoroid Satellite. These data, in the form of payload telemeter signals, were recorded on magnetic tape. To facilitate the reduction of these data, the development of an automatic data readout system, suited both to the special characteristics of the data signals and to the requirements of high-speed digital computing equipment, was initiated at the start of the satellite development program.

As indicated earlier in this report, the telemeter signal is a nonsynchronous time-division multiplex containing information coded in three independent forms: Duration of subcarrier oscillation bursts, frequency of the oscillations, and the time (spacing) between the bursts. The data readout system decommutates and digitizes this information and records the digitized data on magnetic tape in computer format. The readout of data coded in all three forms is simultaneous and is done at a rate of up to 25 channels per second. A major design criterion of the data readout system was that the performance should be satisfactory when there was a significant amount of noise in the telemeter signal.

The design concept of the data readout system included the shared use of digital formatting and tape recording equipment that was a part of other data readout systems in existence at the NASA Langley Research Center.

SECTION II - DATA READOUT SYSTEM

General description.- The block diagram of the data readout system for the Explorer XIII Micrometeoroid Satellite is shown in figure VIII-1. The wave shapes of typical data and control signals, at indicated points, are shown in figure VIII-2. The telemeter data tape is reproduced at 1/16 recorded speed so that the readout rate is within the capability of the formatting equipment. The pulse detection and shaping circuits generate a duration data gating pulse train and a spacing data gating pulse train, both of which lag the input signal by 8 milliseconds. Because of the nonsynchronous nature of the telemeter signal, all of the automatic system control signals are derived from these pulse trains, in addition to representing the basic time-coded data.

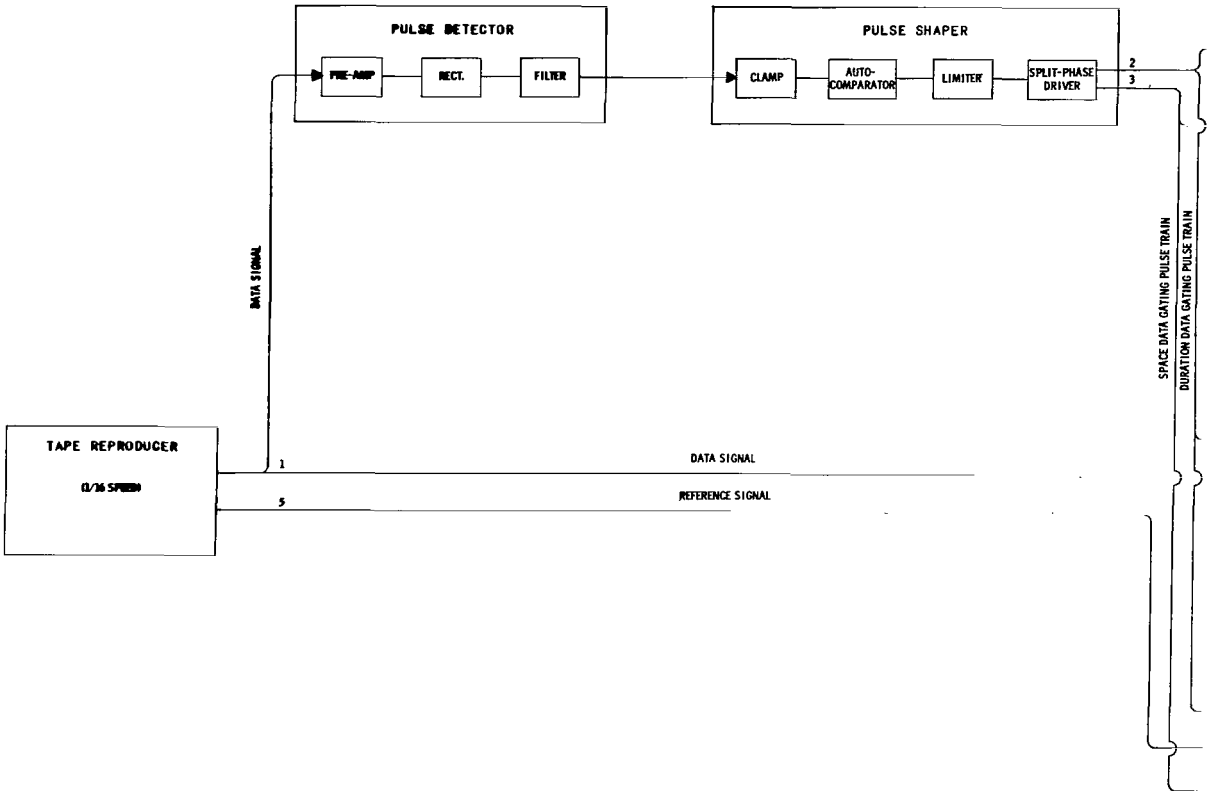
PULSE DETECTOR
PRE-AMP
RECT.
FILTER
PULSE SHAPER
CLAMP
AUTO-COMPARATOR
LIMITER
SPLIT-PHASE DRIVER
2
3
DATA SIGNAL
SPACE DATA GATING PULSE TRAIN
DURATION DATA GATING PULSE TRAIN
TAPE REPRODUCER
1
DATA SIGNAL
5
REFERENCE SIGNAL

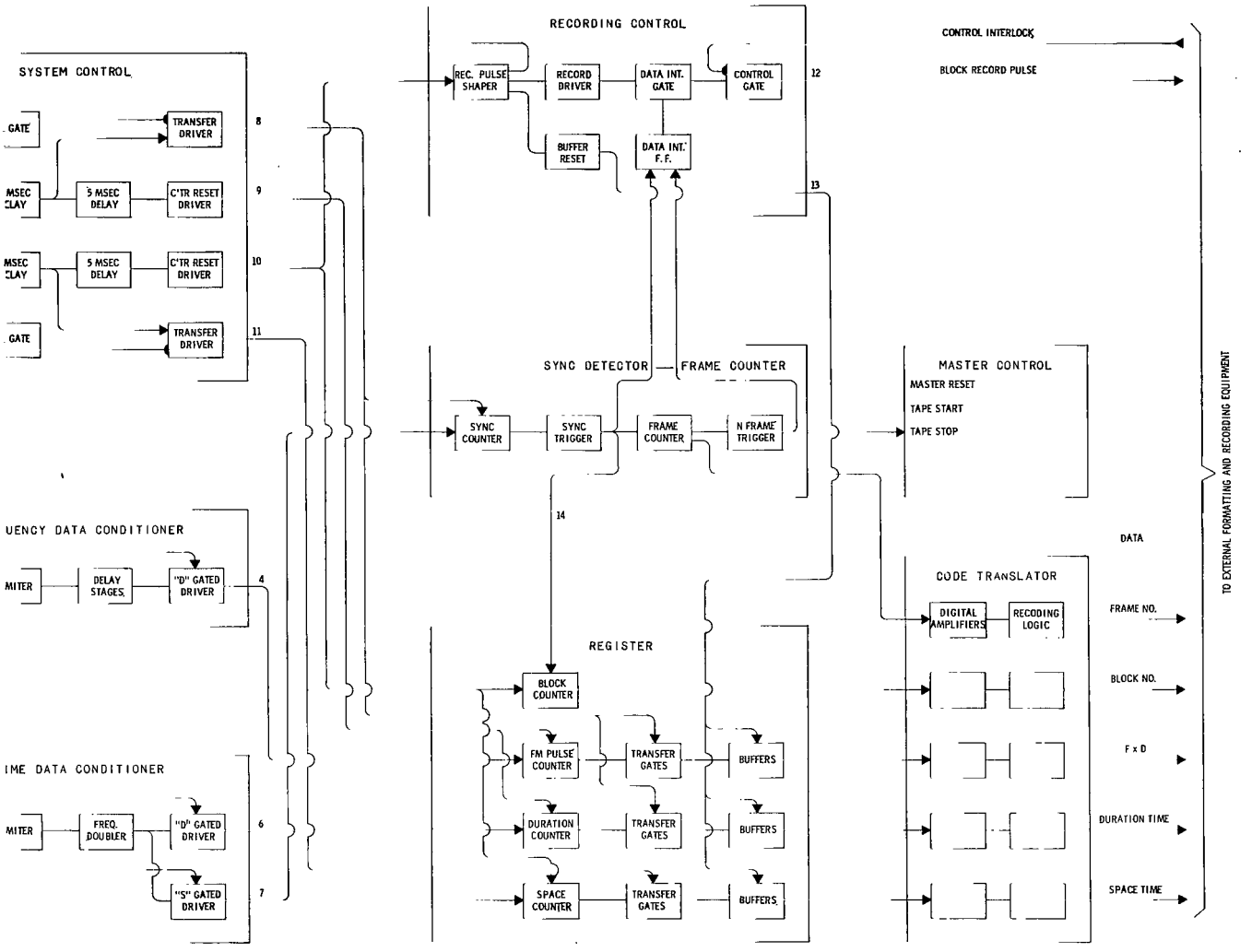

Figure VIII-1.- Block diagram of data readout system.

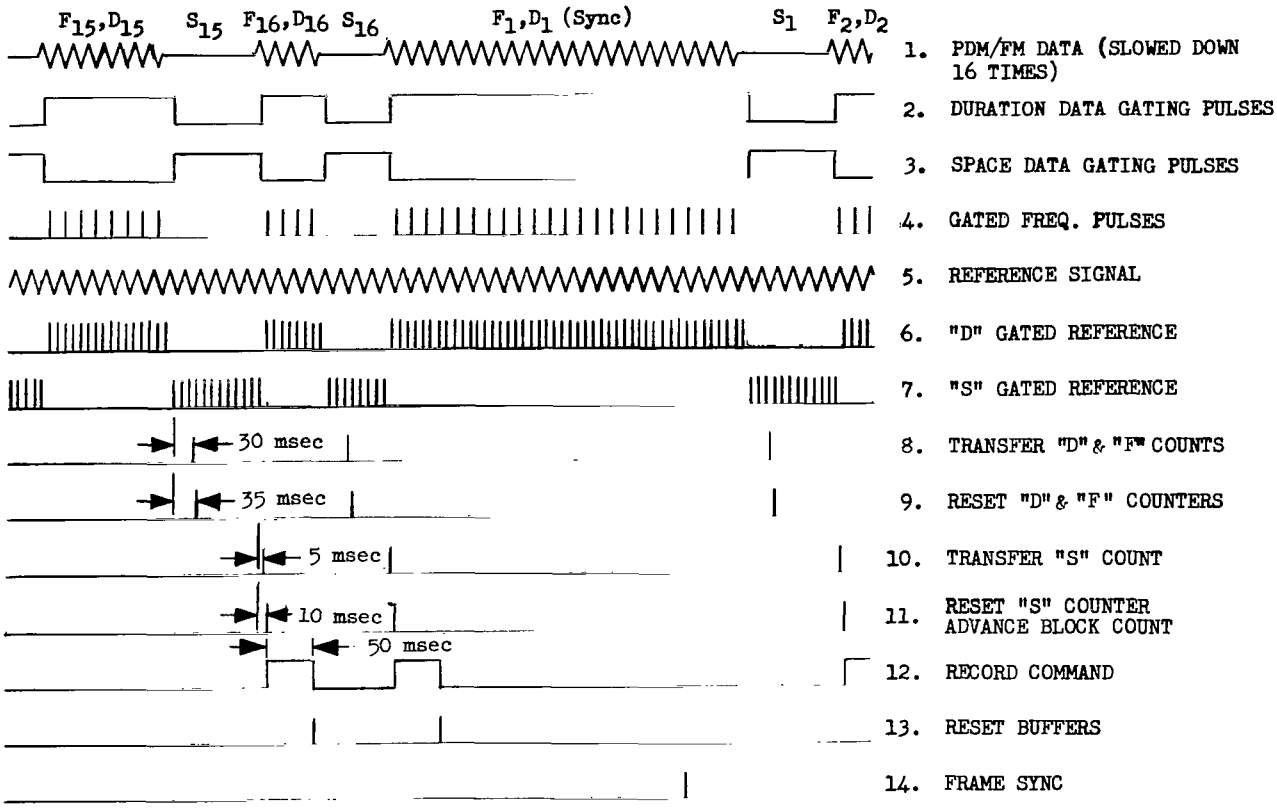

Figure VIII-2.- Data readout system signals.

The durations of the data gating pulses are measured by gating clock pulses into each of two counters. A clock pulse is generated at each zero crossing of a 10-kilocycle (real time) reference signal which had been recorded on one track of the input data tape, thus providing an effective 20-kilocycle clock pulse train. The number of subcarrier cycles in a burst are counted simultaneously with the measurement of the burst duration. Frequency is subsequently computed from these two measurements. The subcarrier cycles are also gated by the duration data gating pulse in order to prevent counting noise cycles. Before gating, the subcarrier pulses are therefore delayed by 8 milliseconds to match the delay of the data gating pulse. The block of data accumulated in the counters during a subcarrier burst and the following space is transferred to a set of three flip-flop buffers at appropriate times (see fig. VIII-2). The data are then recorded on digital magnetic tape as a single block of three channels. A block-identifying counter is advanced just before the initiation of each ditigal readout. Each time frame sync is detected, this counter is reset and a frame-identifying counter is advanced one count. When the block of data being recorded on the digital tape is followed by a block having a minimum burst duration, the second "space" occurs before the recording has been completed. Buffering is therefore required for the "space" data as well as the other data. Since the block and frame counters are not advanced during the recording of a block of data, they do not require buffering.

The timing of control signals 8 to 12, shown in figure VIII-2, is based upon the characteristics of the external digital formatting equipment and an allowance for actual durations and spacings to be as short as 60 percent of the minimum expected from the telemetry encoder. However, as is shown later, false data pulses of very short duration can be generated when the readout system input signal is very noisy. A transfer pulse could then occur either while data were being read out from a buffer or while a counter was active. The result of this transfer would be the recording, on the digital magnetic tape, of an invalid code. To prevent the recording of an invalid code, the transfer of data from a counter to its buffer is inhibited whenever that counter is active or the readout of a block of data is in progress.

The outputs of the buffers and the identification counters are in the 1-2-2-4 code usually required for digital printers rather than the binary coded decimal (BCD) code required by the external digital formatting equipment. Before entering the formatting equipment, the digital data are fed to the code translator (see fig. VIII-1) which changes the bit level voltages and converts the code to BCD. A digital printer, driven directly from the buffers and identification counters, was initially included in the readout system as a quick-look device but it was discarded when the required maintenance outweighed its usefulness.

As was mentioned previously, the readout system utilized digital formatting and tape recording equipment that was a part of existing systems. The signals from the Explorer XIII data readout system were connected via a patchboard network to any one of three Beckmann Inc. Model 210 data recording systems which are operated as a central data recording facility. The outputs of the latter systems are recorded on magnetic tape in IBM 7070 computer format.

Data resolution.- As stated previously, the durations of the data gating pulses are measured by gating 20-kc (real time) clock pulses into counters. The measurement resolution R_t, for the time-coded data are, therefore, the time represented by ±1 count, or ±0.05 millisecond.

The resolution of the measurement of the number of subcarrier cycles N during a burst is also ±1 count. However, the subcarrier frequency is computed by dividing this measurement by the measurement of the independent burst duration D. The computed frequency F_c is:

$$F_c = \frac{\frac{N \pm 1}{20D \pm 1}}{20} \tag{1}$$

but

$$N = F \times D \tag{2}$$

where F is the actual frequency. Therefore:

$$F_c = \frac{20(FD \pm 1)}{20D \pm 1} \tag{3}$$

where F_c and F are in kilocycles and D is in milliseconds. The resolution R_f, of the frequency measurement is:

$$R_f = F - F_c = \frac{\pm F \mp 20}{20D \pm 1} \approx \frac{\pm F \mp 20}{20D} \tag{4}$$

R_f is not, therefore, constant as is R_t.

The rms resolution scatter is determined from the expected distribution of R_f which includes cases of zero resolution error in the measurement of N and/or D, and is given by

$$R_{f,rms} \approx \frac{1}{20D}\sqrt{\frac{2}{3}(F^2 + 400)} \tag{5}$$

The ranges of the telemetric frequency and duration channels were 6 kilocycles to 15 kilocycles and 4 milliseconds to 15 milliseconds, respectively. The expected range of the resolution scatter for the frequency-coded flight data was 0.057 kilocycle, rms to 0.256 kilocycle, rms. Calibrations of the telemetry frequency channels were made with the time channels set at full scale, thereby holding the resolution scatter to a maximum of 0.068 kilocycle, rms.

Noise suppression.- It was expected that, in general, the telemeter signals received from the Explorer XIII Micrometeoroid Satellite would be fairly noisy. The recorded intelligence signal thus appeared as a series of bursts containing subcarrier oscillations and noise. However, the spaces between the bursts contained pure noise, with some noise peaks exceeding the signal peaks even when the rms signal-to-noise ratio was of the order of 7 to 10 decibels. In order to differentiate between the subcarrier bursts and the noise filled spaces under these conditions, the pulse detector was designed as an approximation to a root-mean-square voltage detector. The pulse detector consisted of a preamplifier, rectifier, and filter. The output of this circuit was a pulse train which exhibited the following characteristics. The peaks of the pulses were equal to 90 percent of the rms amplitudes of only the subcarrier oscillations, provided the input-signal-to-noise ratio was greater than +6 decibels. The base level of the pulse train was equal to 70 percent of the rms amplitude of the noise in the "space," provided the noise had a Gaussian distribution. Since the frequency spectrum of a rectified random noise is continuous to zero cps, it was necessary that the filtering after the rectifier be as heavy as possible without imposing an excessive pulse rise time. The filter was chosen so that the pulse rise time (10- to 90-percent amplitude) was 20 milliseconds. Since the input data tapes are played back at 1/16 of the recorded speed, this time corresponds to 1.25 milliseconds, referred to real time. With this filter, some residual noise ripple was present in the detector output signal.

The time between the points at which the detector output signal is halfway between pulse base and pulse peak is equal to the duration of the subcarrier bursts. In order to generate sharp-edged data gating pulses which corresponded to these intervals, the pulse shaper employed a self-referenced amplitude

comparator. The base of the detector output signal was clamped to ground and the clamp circuit output was connected to one input of the comparitor. In addition, the detector output signal, attenuated by 50 percent, was connected to a second clamp circuit which was followed by a long time constant diode detector. This circuit held the reference input of the comparator at one-half the difference between the base and peak levels of the detector output signal. The comparator was designed so that its output was constant until the reference level was exceeded. The remainder of the pulse shaper consisted of a three-stage limiter to provide further pulse shaping and an inverter to provide two data gating pulse trains of opposite phase. These pulses lagged the detector input signal by 8 milliseconds.

In figure VIII-3, the detector input and output signal and one of the shaper output signals are shown for several signal conditions. The rise of the base level of the detector output signal, as the input noise increased, is not evident as it was necessary to adjust the oscilloscope trace of this signal to keep it from overlapping with the trace of the input signal. For noise-free input signals, the shaper output pulses have the same durations as the subcarrier bursts. As the noise in the input signal increases, the residual detector ripple causes some scatter in the durations of the data gating pulses at the output of the pulse shaper. When a residual noise peak is great enough to cross the comparator threshold or when there are rapid variations in the rms noise level which prevent clamping, false data gating pulses are generated. The blocks of data become misnumbered and the resultant loss of synchronization is carried on to the digital magnetic tape. However, the data computing program includes a check of both the block count and the sync channel duration. This check detects the loss of synchronization and causes the entire frame to be rejected.

(a) Mean signal-to-noise ratio, 19.7 decibels.

(b) Mean signal-to-noise ratio, 10.8 decibels.

(c) Mean signal-to-noise ratio, 8.6 decibels.

(d) Mean signal-to-noise ratio, 7.4 decibels.

Figure VIII-3.- Pulse detector and shaper signals.

SECTION III - DATA PROCESSING OPERATIONS

The data readout system previously described and high-speed digital data handling equipment (IBM 7070, 1401, 407-tabulator) were used to process the payload telemeter calibration data and flight qualification test data as well as data received from the orbiting spacecraft.

The computing process for the calibration and qualification data included computation of the subcarrier frequencies. The basic data measurements (frequency, "duration" time, and "space" time) were sorted by channel and frame, and simultaneously listed and plotted on the tabulator. Approximately 711,000 points were processed in this manner during the qualification and calibration of the flight payload telemeters.

Processing of the data telemetered from the spacecraft required two computing and listing operations for each set of data. The result of the first operation was a listing of the mean values of the basic time and frequency measurements of each channel. From these listings, the telemeter identification was verified and the mean values of the calibration channels and the telemeter temperature, which were used in the second operation, were determined.

The computing program for the second operation included the correction of the time multiplexed data for zero and sensitivity changes and selection of the subcarrier oscillator calibrations applicable for the measured telemeter temperature. The physical quantities measured in the various satellite experiments were then computed and were listed as a function of time.

The computing programs for both of the experimental data operations included the detection and rejection of frames in which channel synchronization had been lost. Since tabulator plotting was not required for the experimental data, only the IBM 7070 and 1401 were used in the data processing operations. Approximately 43,000 points of experimental data were processed.

SECTION IV - PERFORMANCE EVALUATION

The performance of the data readout system was evaluated as a function of the quality of the recorded telemeter signal. The mean signal-to-noise ratio and the noise level variation, caused by spacecraft spinning, were measured by recording the output of the signal burst detector (fig. VIII-1). The characteristics which were evaluated were the ability to maintain channel synchronization (i.e., identification) and the reading scatter.

Table VIII-1 lists the interrogation history of the spacecraft telemeters. The recorded data which, after preliminary oscilloscope monitoring were judged to be automatically readable to any extent, are indicated. The range of the measured signal-to-noise ratios of these data recordings was from 7.4 to 19.7 decibels.

The data readout system was programed to read out 50 frames of data from each telemeter record. In cases where frame sync was not detected in each frame, the number of telemeter frames that were processed was greater than 50. For these cases, the exact number of frames was determined from the reading of a block counter in the digital formatting equipment. In figure VIII-4, the percentage of frames for which complete channel synchronization was maintained is plotted as a function of the mean signal-to-noise ratio, in decibels, of the telemeter signal. The data readout system has a pronounced "performance threshold" at a signal-to-noise ratio of approximately 10 decibels. For input signal-to-noise ratios between 10 and 20 decibels, channel synchronization is maintained for an average of 90 percent of the telemeter frames. Automatic readability performance of 100 percent could be expected for input signal-to-noise ratios on the order of 40 decibels.

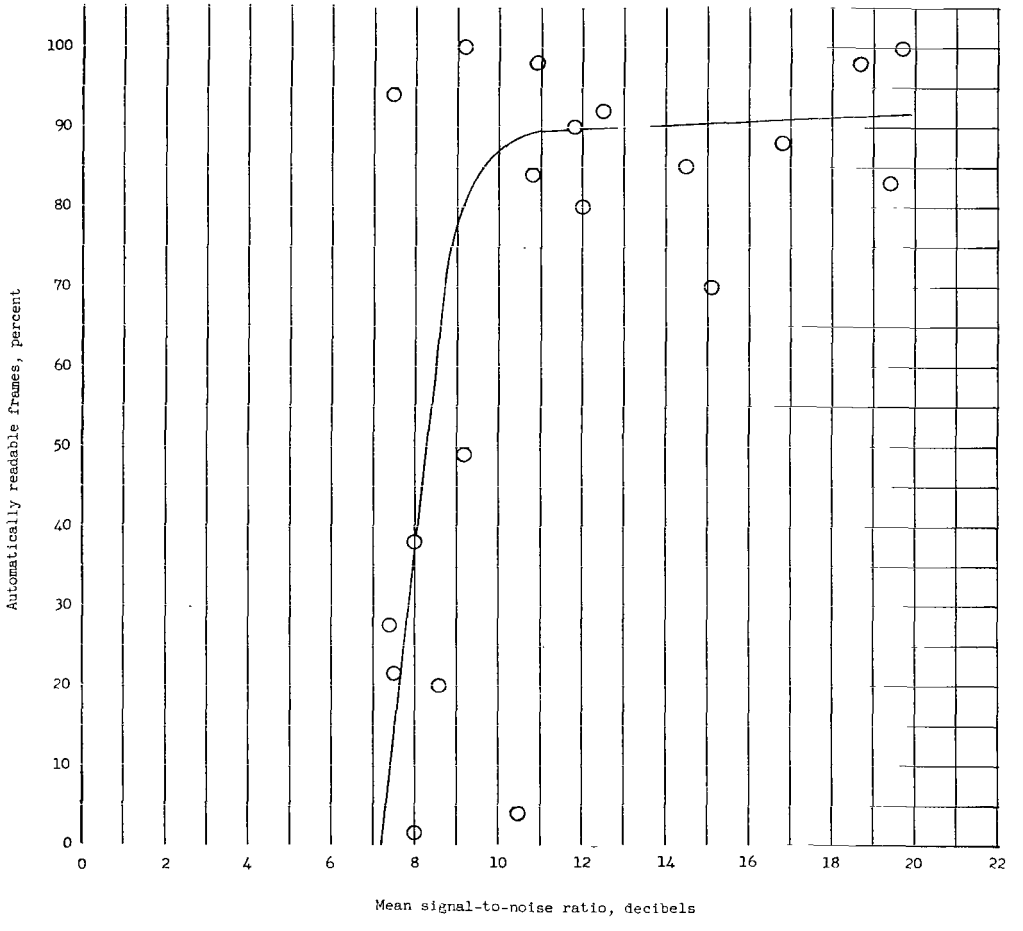

Figure VIII-4.- Detection performance of data readout system.

Figure VIII-5 is a plot of the root-mean-square reading scatter of the time-coded data as a function of the mean signal-to-noise ratio of the data signal. The results are shown for signal-to-noise ratio greater than the performance threshold which is evident in figure VIII-4. Below this level the

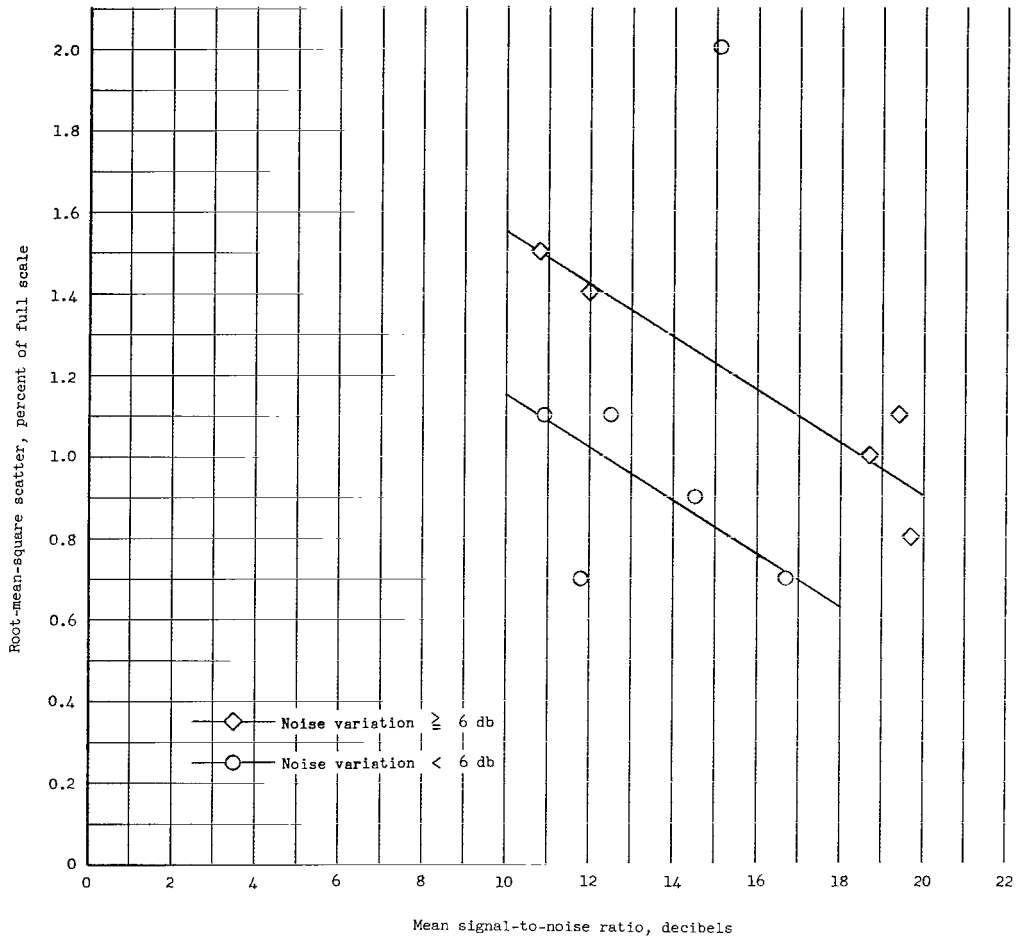

Figure VIII-5.- Reading scatter; time-coded data.

number of readings available were, in general, not sufficient for a statistically significant calculation of the rms scatter. The effect of the fluctuations in noise level is indicated by classifying the results as to whether the noise level variation was less than 6 decibels or greater than 6 decibels. At the threshold, the rms scatter levels are 1.1 and 1.5 percent of full scale, respectively. For the range of signal quality encountered, the scatter decreases linearly with increasing signal-to-noise ratio. If the linearity should continue beyond this range, the reading scatter would be expected to reach the basic resolution limit (rms scatter, 0.37 percent of full scale) at 22 decibels and 30 decibels.

As previously shown, the resolution scatter of the data readout system, for frequency measurement, is a variable which reaches a significant level under conditions of high subcarrier frequency and coincident low burst duration. The performance of the system for frequency coded data was therefore evaluated by determining the ratio of the measured scatter to the expected resolution scatter. The results are shown in figure VIII-6 and represent the group correlation for

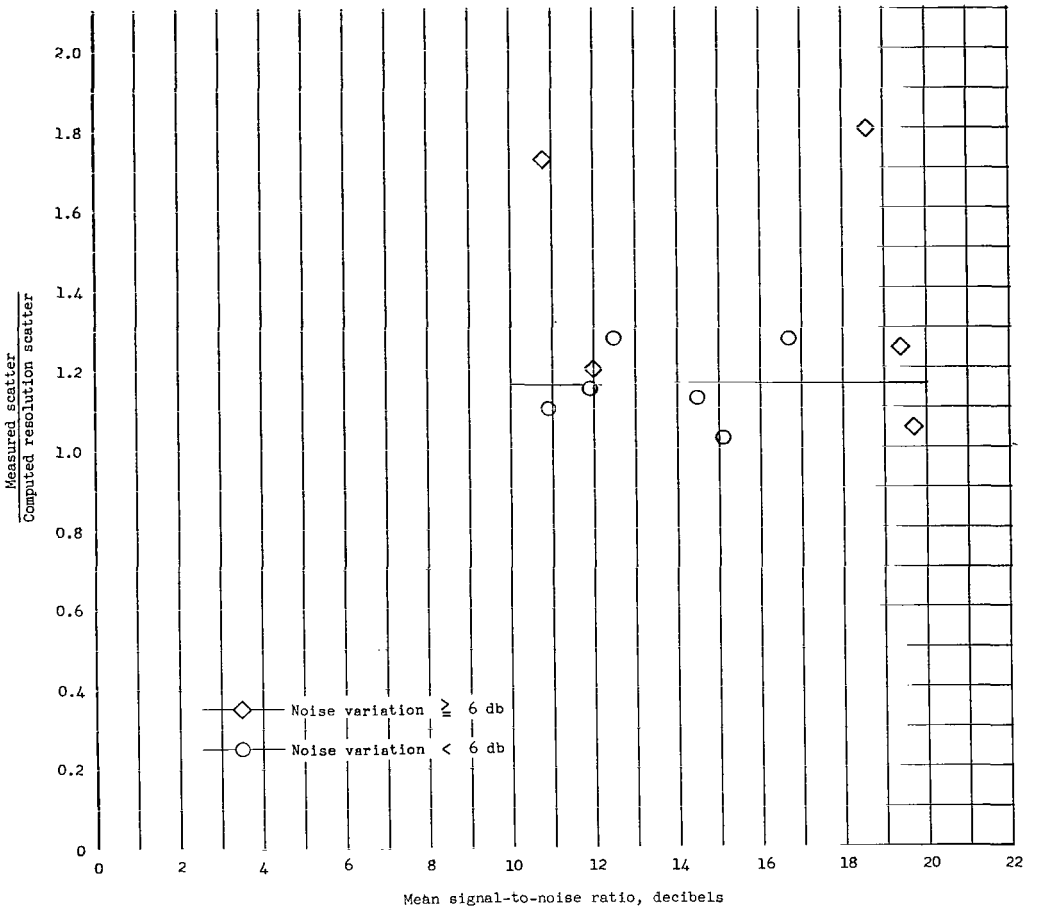

Figure VIII-6.- Scatter correlation; frequency-coded data.

all of those channels for which nonvariance of the subcarrier oscillators could be assumed. The expected group resolution scatter σ_N was calculated from the equation

$$\sigma_N = \sqrt{\frac{\sigma_1^2 + \sigma_2^2 + \cdots + \sigma_n^2}{n}} \qquad (6)$$

where σ_1, σ_2, $\cdots$ σ_n are expected scatter values for each channel. For the range of signal-to-noise ratios encountered, the average correlation was 1.16, indicating only minor degradation of performance due to noise. The two points for which the correlation is 1.8 and 1.7 correspond to interrogations of the "B" telemeter near the end (orbits 23 and 28) of the orbiting lifetime of the satellite.

TABLE VIII-1.- ORBITAL TELEMETRY HISTORY

Orbit	Date/Time	Minitrack station	Tape	Telemeter	Data-reduction process
Launch	25/18:29:44	Blossom Point	122A001	None	None
1	25/20:11:45	Grand Forks	122N001	B	Automatic
1	25/20:11:45	Blossom Point	122A002	B	Automatic
1	25/20:17:14	Blossom Point	122A002	A	Manual*
2	25/21:59:40	Fort Myers	122D001	None	None
7	26/06:34:00	Santiago	122J001	None	None
8	26/08:32:15	Santiago	122J001	None	None
9	26/10:02:40	Antofagasta	122H001	A	Manual
9	26/10:02:40	Antofagasta	122H001	B	Manual
10	26/11:46:00	Quito	122F001	A	Manual
10	26/11:55:00	Quito	122F001	B	Manual
13	26/15:13:30	Fort Myers	122D001	A	Automatic
13	26/15:15:02	Fort Myers	122D001	B	Automatic
13	26/15:13:30	Blossom Point	122A003	A	Automatic
13	26/15:15:02	Blossom Point	122A003	B	Automatic
14	26/16:58:06	Blossom Point	122A004	A	Automatic
14	26/16:58:06	Blossom Point	122A004	B	Automatic
14	26/16:58:06	Fort Myers	122D002	A	Automatic
14	26/16:58:06	Fort Myers	122D002	B	Automatic
15	26/18:40:57	Fort Myers	122D002	A	Automatic
15	26/18:40:57	Fort Myers	122D002	B	Automatic
20	27/03:03:00	Santiago	122J002	A	Manual
20	27/03:03:00	Santiago	122J002	B	None
21	27/04:45:56	Santiago	122J003	A	Automatic
21	27/04:45:56	Santiago	122J003	B	Automatic
22	27/06:21:30	Santiago	122J003	A	Automatic
22	27/06:21:30	Santiago	122J003	B	Automatic
23	27/08:03:14	Antofagasta	122H001	A	Automatic
23	27/08:03:14	Antofagasta	122H001	B	Automatic
25	27/11:15:40	Lima	122G01	None	None
27	27/14:03:00	Woomera	122-1	None	None
28	27/15:42:15	Woomera	122-1	A	Automatic
28	27/15:42:15	Woomera	122-1	B	Automatic
35	28/02:00:03	Antofagasta	122H001	A	Manual**
35	28/02:00:03	Antofagasta	122H001	B	Manual**
40	28/08:46:00	Antofagasta	122H001	B	Manual**

*Special Process by GSFC.

**The temperatures of all systems had increased beyond design limits as a result of aerodynamic heating so that these data could not be used.